



The performance of Perovskite solar cells with silicon carbide as an interfacial layer

Dena N Qasim Agha

Qais Th. Algwari

Ninevah University / College of Electronics Eng. / Dept. of Electronic

(Received in 15/7/2021 accepted in 1/9/2021)

Abstract:

The current work involved the numerical simulation of investigating the impact of conduction band offset (CBO) on the perovskite solar cell parameters. The solar cell structure under investigation comprises the (Spiro OMe TAD), ($\text{CH}_3\text{NH}_3\text{PbI}_3$), and (SnO_2) as HTL, the absorber layer, and ETL with electron affinities (χ) of (-2.45, -3.9, and -3.75) eV respectively. The conduction band alignment was controlled by inserting an interfacial layer between the absorber and ETL. The inserting layer is a thin layer of 3C-SiC material. Before utilizing the interfacial layer, a parametric study was attained, which included the doping variation and thickness variation of each layer. According to the findings, the device performs best at a thickness of 200 nm, 400 nm, 300 nm for HTL, perovskite absorber layer, and ETL respectively, with a doping concentration of 10^{19} cm^{-3} , 10^{14} cm^{-3} , and 10^{19} cm^{-3} for the same layers. These parameters provide a J_{sc} , V_{oc} , FF, and PCE of 26.1 mA.cm^{-2} , 1.11 V, 83.23%, and 24.19% respectively. Utilizing 3C-SiC as an interfacial layer with thickness 100 nm and doping 10^{18} cm^{-3} improved the performance of the device. According to the electron affinity for the proposed structure (the absorber layer and ETL) with the interfacial layer produce spike-spike band alignment. The results showed that the spike-spike band structure with ($\Delta\chi_1= 0.07$) eV for absorber layer with 3C-SiC and ($\Delta\chi_2=0.08$) eV for 3C-SiC interfacial layer and SnO_2 as ETL, produces a good improvement in the cell performance with an increase in PCE (from 24.19 % to 28.36 %).

Keywords: Perovskite solar cells, Conduction band offset (CBO), Electron affinities, 3C-SiC and interfacial layer.

تأثير محاذاة حزمة التوصيل على أداء خلايا البيروفسكايت الشمسية

دينا نمير قاسم أغا
قيس ذنون الجواري
جامعة نينوى / كلية هندسة الإلكترونيات / قسم هندسة الإلكترونيك

ملخص البحث:

تضمن العمل الحالي على المحاكاة العددية للتحقيق من تأثير الإزاحة في حزمة التوصيل (CBO) على معاملات خلية البيروفسكايت الشمسية. حيث تكون هيكل الخلية الشمسية من ثلاث طبقات وهي (Spiro OMe TAD) و $(\text{CH}_3\text{NH}_3\text{PbI}_3)$ و (SnO_2) تمثل الطبقة الناقلة للفجوات (HTL) والطبقة الماصة والطبقة الناقلة للإلكترونات (ETL) ذات الفئة الإلكترونية بقيم $(-2.45$ و -3.9 و -3.75 eV) على التوالي. حيث تم التحكم في محاذاة حزم التوصيل عن طريق إدخال طبقة بينية بين الطبقة الماصة وطبقة نقل الإلكترونات من مادة 3C-SiC. تم إجراء دراسة بارامترية تضمنت التحقق من تركيز ذرات التشويب والسّمك للطبقات الثلاث. وفقاً للنتائج، تعمل الخلية المقترحة بشكل أفضل عند سماكة 200 نانومتر و 400 نانومتر و 300 نانومتر للطبقة الناقلة للفجوات (HTL) و الطبقة الماصة البيروفسكايت و طبقة نقل الإلكترونات على التوالي، في حين تم الوصول إلى استخدام تركيز ذرات التشويب بقيم 10^{19} سم⁻³، 10^{14} سم⁻³ و 10^{19} سم⁻³ لنفس الطبقات المذكورة سابقاً. و بعد ذلك أصبحت المعاملات للخلية الشمسية Jsc و Voc و FF و PCE تبلغ 26.1 مللي أمبير سم⁻² و 1.11 فولت و 83.23% و 24.19% على التوالي. بعد ذلك أدى استخدام طبقة رقيقة من 3C-SiC كطبقة بينية بسّمك 100 نانومتر ومقدار تركيز ذرات التشويب بلغ 10^{18} سم⁻³ إلى تحسين أداء الخلية. وفقاً لتقارب الفئة الإلكترونية للهيكल المقترح (الطبقة الماصة و طبقة نقل الإلكترونات ETL) مع الطبقة البينية تم إنتاج محاذاة حزمة توصيل نوع قمة-قمة. وعليه نتج عن ذلك $(\Delta\chi_1=0.07$ eV) للطبقة الماصة مع الطبقة البينية ومن ثم $(\Delta\chi_2=0.08$ eV) للطبقة البينية و $\text{ETL} \leq \text{SnO}_2$ ، فنتج زيادة في نسبة الكفاءة PCE (من 24.19% إلى 28.36%).

1. Introduction

Perovskite solar cells (PSC) were discovered by Japanese scientists Kojima *et al.* in 2009. The power conversion efficiency (PCE) of only 3.8 % and their stability was poor [1]. The interest in PSC was started in 2012 when Grätzel *et al* succeeded to get the PCE to 9.7% with 500 hours of stability [2]. It consists of a transparent electrode on a glass surface, such as indium tin oxide (ITO) or fluorine-doped tin oxide (FTO), and an electron transportation layer on the ITO/FTO (ETL). The perovskite layer is the active layer that sits on top of the ETL, where light photons are absorbed and an electron-hole pair is excited. Then, the hole transporting layer (HTL) is placed on top of the perovskite, followed by a metallic electrode. A closed-circuit cell is formed by connecting the transparent electrode and the metallic electrode as shown in Figure (1). All layers of the structure have been subjected to research and development, as each layer contributes to the increase in PCE. The ETL has gotten a lot of attention because of its ability to significantly improve cell performance by collecting electrons more efficiently and preventing electron-hole recombination [3][4][5]. The charge selectivity and collection efficiency of the ETL and HTL are what distinguish them. Efficient charge collection results in ideal current-voltage behavior and increases power conversion efficiency (PCE). As a result, a variety of interfacial engineering strategies for avoiding major interfacial issues such as energetic alignment, charge transfer, charge accumulation, recombination, and extraction have been proposed [6]. Different materials can be used as ETL and as HTL but the most commonly used for ETL are (SnO₂, CdZnS, PCBM, TiO₂, IGZO, and CdS) [7], and for HTL the most common one is Spiro-OMe TAD [8]. The generated charge carriers by photon interaction in the absorber occur when the light energy higher than the semiconductor bandgap, and these carriers will drift to interface regions at the HTL-perovskite and ETL-perovskite borders under the effect of the built-in potential. Because of the energy barrier and/or poor charge transport of the HTL or ETL, charges will accumulate at the interface of these layers, increasing charge recombination and lowering solar cell efficiency. To avoid the aforementioned issue, the energy band alignment should be carefully engineered. The results of the last study [9] showed that the 3C-SiC interfacial layer gave the better performance of the solar cell, consequently, the study of the current work focused on chosen the 3C-SiC layer as an interfacial layer between MAPbI₃ and SnO₂ as ETL. In the present work, because of the band match, the added layer should improve charge transfer

across the layers and reduce electron energy losses during transportation, resulting in improved solar performance.

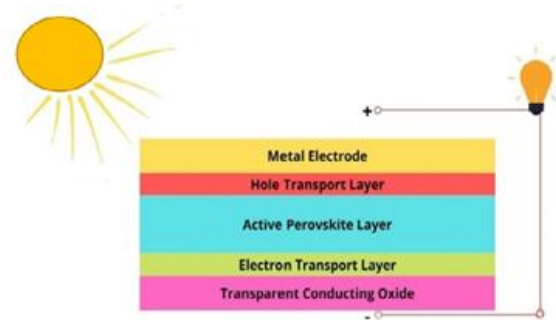


Fig (1). The layers of perovskite solar cells.

2. Methodology

The modeling calculations presented in the following section were performed using the free solar cell software Solar Cells Capacitance Simulator in One Dimension (SCAPS-1D), developed by researchers at the University of Ghent, Belgium [10], and version 3.3.01 was used in the current work [11]. The fundamental equations for semiconductor device activity describe the static and dynamic behavior of carriers in semiconductors when external effects such as applied fields or optical excitation cause a deviation from thermal equilibrium [12]. These are the equations:

The term Poisson's equation refers to the relationship between potential and charges in space. The electric field (E) in the device is affected by the current flowing and charges in delocalized states, traps, and recombination centers, as shown in Eq (1).

$$\frac{d}{dx} \left[\epsilon(x) \frac{d\psi}{dx} \right] = q [p(x) - n(x) + N_d(x) - N_a(x) + p_t(x) - n_t(x)] \quad (1)$$

Where ϵ represents relative permittivity; q is the electron charge, N_a is the ionized acceptor density and N_d is the ionized donor density while ψ representing the electrostatic potential. The term x signifying the coordinate position; and both of n_t and p_t , represent respectively the number of trapped of electrons and holes [7][13].

The term "continuity equations" refers to the transportation of carriers for electrons (Equation (2)) and holes (Equation (3)) embedded in SCAPS.

$$-\frac{1}{q} \frac{dJ_n}{dx} = G(x) - R_n(x) \quad (2)$$

$$\frac{1}{q} \frac{dJ_p}{dx} = G(x) - R_p(x) \quad (3)$$

Where sJ_p , J_n , $R_p(x)$ and $R_n(x)$ represent, respectively, the current density, and the recombination rates of holes and electrons, while $G(x)$ is the optical generation rate [7].

Figure 1 depicts the proposed solar cell's considered structure. The electron transport layer is SnO_2 , the absorber layer is $\text{CH}_3\text{NH}_3\text{PbI}_3$, and the hole transport layer is the Spiro-OMe TAD. The parameters and the initial values of doping and thickness for the proposed structure are summarized in Table (1) [7] [14] [15] these literatures were used to get the initial values for the proposed structure. The current study used standard conditions, such as illumination with the AM1.5G solar spectrum, a 100 mW.cm^{-2} incident power density, and a temperature of $300 \text{ }^\circ\text{K}$. The ETL, perovskite absorber layer, and HTL absorption coefficients are defined in the simulation program.

Table (1). Illustrates the input parameters for the proposed structure materials (Initial values).

Parameters	SnO_2	$\text{CH}_3\text{NH}_3\text{PbI}_3$	Spiro OMe TAD
Thickness (nm)	90	200	700
The energy Band gap (eV)	3.6	1.55	3.0
Affinity of electron (eV)	3.75	3.9	2.45
Permittivity constant	100	10	3
CB effective density of states ($1/\text{cm}^3$)	2.2×10^{18}	2×10^{18}	2.2×10^{18}
VB effective density of states ($1/\text{cm}^3$)	1.8×10^{19}	2×10^{19}	1.9×10^{19}
Thermal velocity for electron (cm/s)	10^7	10^7	10^7
Thermal velocity for hole (cm/s)	10^7	10^7	10^7
Electron mobility (cm^2/Vs)	240	1.0	0.2×10^{-3}



Hole mobility (cm ² /Vs)	240	1.0	0.2×10 ⁻³
Shallow uniform donor density N _D (1/cm ³)	10 ¹⁷	10 ¹³	–
Shallow uniform acceptor density N _A (1/cm ³)		–	1×10 ¹⁸

Furthermore, due to its basic properties that make it ideal in a variety of situations, silicon (Si) is the most widely used material in electrical devices. Nonetheless, there are limitations with Si, such as the fact that the reduction process may render silicon inefficient at high temperatures. A main issue was the ability to handle the necessary operating conditions. This means that silicon-based devices are not suitable for usage at temperatures above 250°C. With SiC, however, it may be able to operate at temperatures higher than this because of its wide band-gap.

The indirect and wide band gap of Silicon carbide (SiC) (>2.0 eV) and the excellent properties, including a high conductivity, high electron mobility, drift velocity saturation, high thermal stability, good chemical resistance, high breakdown voltage, and good thermal conductivity in addition to the excellent oxide structure capability make them a good alternative to Si in the field of semiconductor application. Silicon Carbide is available in 250 polytypes, with the difference being the stacking. The most commonly used polytypes is 3C-SiC or β-SiC [16] [17] [18]. Also, the electron affinity of 3C-SiC is 3.83 eV [19] consequently for these properties a thin layer of β-SiC was candidate to use as an interfacial layer between absorber layer and ETL in the present work.

3. Results and discussion

A parametric investigation for the proposed solar device structure was carried out to obtain the best performance. A parametric study involved the doping variation and thickness variation. The doping of each layer in the solar cell structure is critical in determining the electrical characteristics and solar cell performance. To exam the influence of the acceptors in HTL on the cell performance, the concentration N_a was varied from 10¹⁷ cm⁻³ to 10²² cm⁻³. Figure (3) illustrates the impact of the examined range of acceptor doping density on the solar cell performance. It can be noticed that the efficiency and fill factor increase with increasing the acceptor doping density but above doping of 10¹⁹ cm⁻³, it saturates. Figure (3) reveals that both J_{sc} and V_{oc} are nearly constant and unaffected by the concentration

of acceptor. This means that doping density does not affect the recombination rate. As it was found by Jeyakumar *et al* [20], that the minority carrier density is affected by the recombination rate, so at high acceptor doping concentration in HTL, the minority carrier density decreases. The increase in the FF and PCE at doping densities greater than 10^{19} cm^{-3} could be explained by an increase in conductivity in HTL at a high doping rate [20]. When the acceptor doping density is $>10^{19} \text{ cm}^{-3}$, good cell performance can be expected.

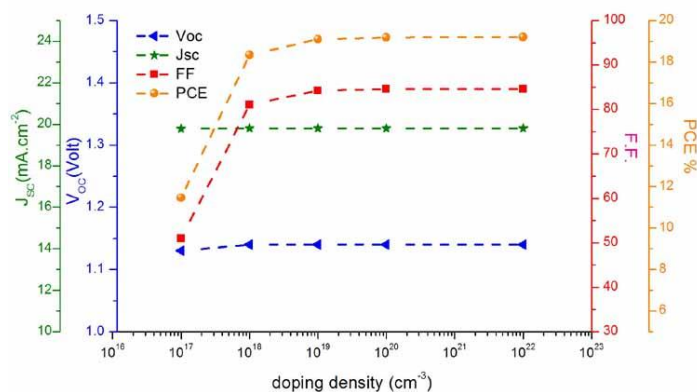
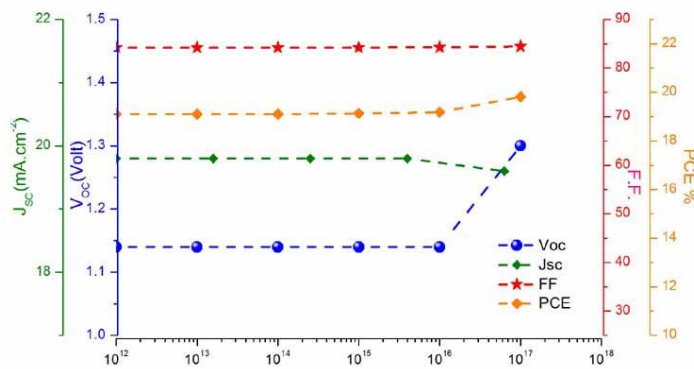


Fig (3) The effect of doping variation for HTL on the solar cell parameters.

The effect of doping density in the absorber layer on cell performance was examined by adjusting the doping density from 10^{12} cm^{-3} to 10^{19} cm^{-3} while keeping the HTL doping density at 10^{19} cm^{-3} . The change in cell parameters as a function of doping density is represented in Figure (4). The cell performance remained virtually unchanged for doping densities below 10^{16} cm^{-3} , as can be seen. Above this value of doping density, the results of device parameters show instability in the cell performance. The reason for this is that high doping reduces the depletion region, which improves the recombination process at the absorber bulk [21]. According to the current findings, the perovskite absorber layer doping concentration ($>10^{16} \text{ cm}^{-3}$) was unsuitable for high performance.



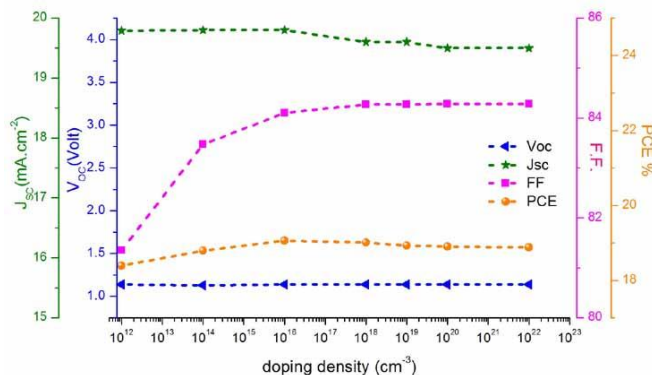


Fig (5) **The effect of** doping variation for the ETL **on the solar cell** parameters.

To examine the influence of ETL doping on solar cell parameters, the doping density of ETL was changed from 10^{17} cm^{-3} to 10^{22} cm^{-3} while the doping density of HTL and perovskite layer are kept at the values of 10^{19} cm^{-3} and 10^{14} cm^{-3} , respectively that have the best stable cell output.

The effect of ETL doping concentrations on the performance of PSCs is shown in Figure (5). It can be noticed that doping causes by the majority of carriers, which leads to the **slightly enhancement in FF and there's no influence impact on the other parameters**. With the moderate doping levels, **slight** improved carrier transport and suitable energy position can be obtained. Increased doping of ETL improves the interface electric field between the ETL and HTL, this raised electric potential used to separate the excitons with less recombination rate and the performance of the device is the **slightly** improved. Otherwise, moderate doping is needed heavy doping causes recombination to rise, and the semi-conductive character of perovskites changes to metallic, obstructing the carrier transport

mechanism [22]. The variation of PV characteristics with ETL doping concentration (cm^{-3}) is shown in Figure (5).

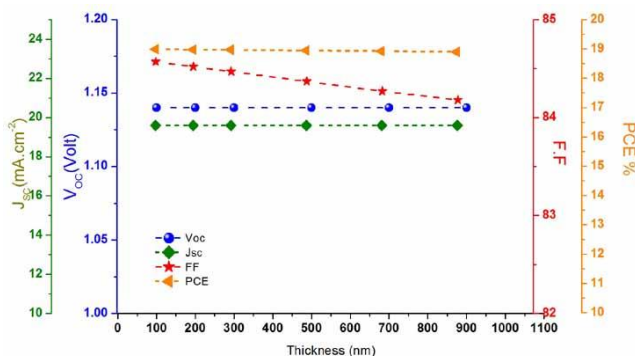


Fig (6) The impact of HTL thickness on the device parameters.

Simulations were run to determine the best thickness of each layer while keeping the doping density of the three perovskite layers at the optimum value that provides the optimum solar cell performance from the previous section. The impact of HTL thickness variation on the proposed solar cell performance was investigated by varying the thickness of the HTL from 100 nm to 900 nm with an increment step of 200 nm. Figure (6) demonstrates that the thickness variation of this layer has no significant effect on solar cell performance. This finding is consistent with Hima *et al* [15], and it can be explained by the fixed quantity of charged carriers formed in the perovskite layer. The thickness of 200 nm was chosen for this layer as an optimum thickness.

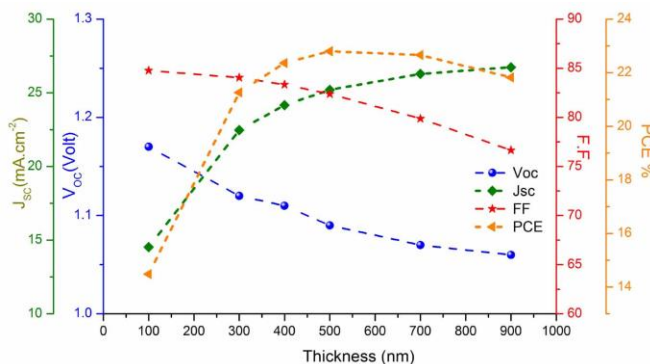


Fig (7) The impact of ETL doping concentration on the device parameters.

The absorber layer thickness was increased from 100 nm to 900 nm to achieve the finest absorption of the incident light in the perovskite layer and thus improve the production procedure of both electrons and holes. Figure (7) shows how the device parameters changed as the perovskite absorber layer thickness increased. Over the observed thickness range, J_{sc} increased from 14.52 mA.cm^{-2} to 26.73 mA.cm^{-2} , while V_{oc} decreased slightly from 1.17 V to 1.06 V. Even though the FF dropped from 84.76 % to 76.66 %, the absorber thickness has a noticeable impact on the efficiency. The efficiency of the cells increased from about 14 % to about 21%, as shown in Figure (7). This enhancement can be attributed to the layer's photo absorption improvement. This means that the total amount of absorbed photons was related to the amount of photo-generated carriers, causing in a J_{sc} rise as layer thickness grows. In other words, the J_{sc} value rises. As the absorber layer thickness increase, i.e, absorbing more photons. Consequently, as the excess carrier concentration, the J_{sc} increases as well. The photo-generated carriers in the absorber layer's center would recombine as the absorber layer's thickness exceeded the diffusion length. This is reflected in the V_{oc} as the effective band gap narrowed and recombination processes increased [22] [23]. However, as the thickness of the absorber layer increased, the solar cell's series resistance and internal power depletion increase as well, significant decrease in FF [7]. The results showed that the performance improved to about 22 % with a better thickness of 400 nm where the solar cell parameters are, respectively J_{sc} , V_{oc} , and FF of 24.16 mA cm^{-2} , 1.11 V, and 83.33 %.

The impact of the ETL thickness variation on the solar cell parameters are shown in Figure (8), where the absorber and HTL thicknesses were kept at the best values that gave the best device performance. It can be noticed that there is not worthy influence of electron

transport layer thickness variation on V_{oc} and FF, however, the J_{sc} and PCE are increased with its thickness increasing.

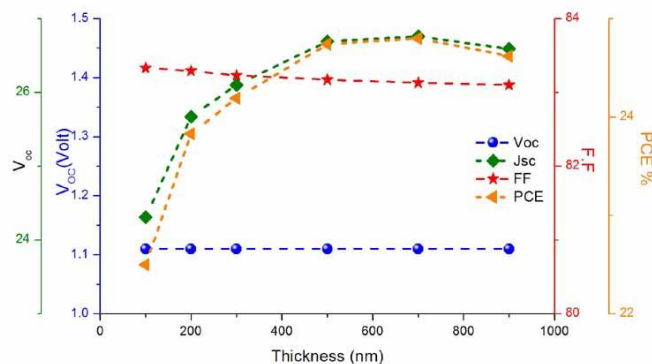


Fig.(8) Impact of ETL thickness variation on the solar cell parameters.

The effect of changing the thickness of the ETL on performance parameters of the solar cell can be ascribed to that the increasing in the thickness of this layer reduces charge accumulation, which in turn reduces recombination. At a thickness of 300 nm, the best findings were achieved [15]. Table (2) summarized the optimized design parameters which will use for the reference solar cell in this current study.

Table (2) illustrates the optimum thickness and doping of the present structure that gives the best cell performance. For these optimum vales the corresponded cell parameters are shown in Table (3).

Table (2). Optimum thickness and doping variation for each material.

Parameters	SnO ₂	CH ₃ NH ₃ PbI ₃	Spiro-OMe-TAD
Thickness (nm)	300	400	200

Shallow uniform donor density N_D ($1/cm^3$)	1×10^{19}	1×10^{14}	1×10^{19}
--	--------------------	--------------------	--------------------

Table (3) The PSC parameters for the proposed structure.

Device parameters	Before optimum	After optimum
V_{oc} (V)	1.14	1.1
J_{sc} $mA.cm^{-2}$	19.61	26.1
FF%	81.12	83.23
PCE%	18.19	24.19

To control the conduction band alignment between the absorber and electron transport layer where conduction band offset CBO between the absorber and the ETL could be a spike band offset or cliff band offset. The spike structure is formed when the conduction band of ETL is higher than the conduction band of the perovskite absorber, i.e. CBO (+). This structure acts as a barrier to the electrons passing from the absorber layer to ETL. In contrast, the conduction band energy would a cliff, i.e. CBO (-) which has no potential barrier formed, when the conduction band of ETL is lower than that of the absorber layer [24] as shown in Figure (9).

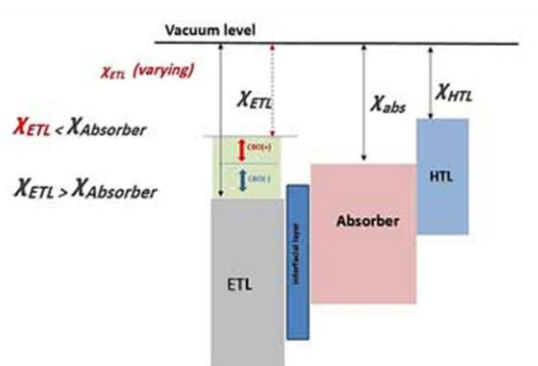


Fig. (9) General band alignment scheme of main layers at PSCs.

$\Delta\chi_1$ and $\Delta\chi_2$ are defined as CBO between the absorber/interfacial layer and interfacial layer/ETL respectively, so through using a layer of 3C-SiC, with electron affinity of -3.83 eV [19] as an interfacial layer between the absorber layer and the ETL (SnO_2) produce a spike band offset structure was formed between the absorber and 3C-SiC layer with $\Delta\chi_1 = +0.07$ eV. Meanwhile, the value of $\Delta\chi_2 = +0.08$ eV was formed between the 3C-SiC layer and SnO_2 . Figure (10) shows J-V curve for the reference cell and the cell with the existence of an interfacial layer. It can be noted that there is a noticeable enhancement in J_{sc} where it is increased from 26.1 mA.cm^{-2} to 30.48 mA.cm^{-2} . The inserted layer affects slightly the FF where its value is enhanced from 83.13% to 83.23% while the V_{oc} is not changed. The increase in J_{sc} is noticeably reflected on PCE where it is raised from 24.19% to 28.36%. The corresponding photovoltaic parameters and the average values after adding 3C-SiC layer are summarized in Table (4).

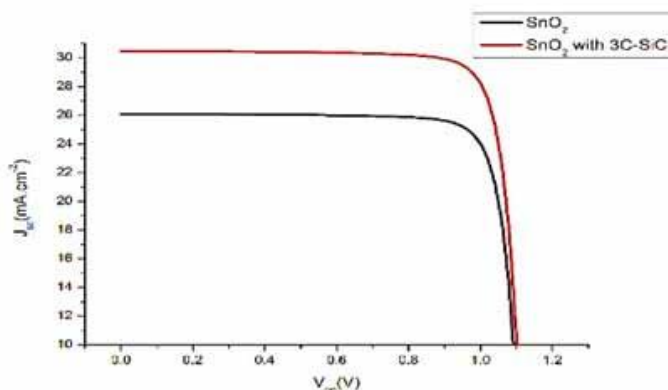


Fig. (10). J-V curve for SnO_2 before and after utilizing 3C-SiC layer.

Table (4). Device performance after adding an interfacial layer.

Device parameters	After adding 3C-SiC
V_{oc} (v)	1.1

J_{sc} (mA.cm ⁻²)	30.48
FF %	83.13
PCE %	28.36

The simulation results show that inserting the 3C-SiC as an interfacial layer with proper electron affinity between the absorber and ETL produces an enhancement in the solar cell performance relative to the reference cell regardless of the electron affinity. To determine the better band alignment structure that gives the best PSC output. However, there was an evident enhancement with 3C-SiC with regards to cell parameters. On the subject of the cell performance, the V_{oc} variation is almost similar for this structure; that was about 1.1 V. This could be due to the relatively unchanged R_{sh} value with the utilization of the interfacial material. Furthermore, there was an improvement in the J_{sc} after 3C-SiC was utilized as an interfacial layer. It was also noticed that the maximum current was 30.48 mA.cm⁻² at the structure with SnO₂ as ETL, i.e at spike-spike energy alignment. It was also found that the J_{sc} curve behaved relatively similarly for the cell structure before and after the addition of 3C-SiC layer, but with distinctly higher values of J_{sc} seen after the addition of the interfacial layer. This behavior could be attributed to the decrease in the recombination process. Meanwhile, the FF value was found to be relatively constant compared to its initial value, A possible explanation to this finding could be that the addition of 3C-SiC layer exerted no effects on the R_s . Finally, according to the yielded findings after the insertion of the 3C-SiC layer, it was obvious that the PCE was increased compared to the reference cell structures. The justification of this behavior could be the fact that there is less recombination process at the border between the absorber layer and ETL [24] [25]. The 3C-SiC improved the device performance for the spike-spike structure.

4. CONCLUSIONS

Based on SCAPS software the present work involved the study of the role of the conduction band alignments on the perovskite solar device performance. The proposed structure of the cell under investigation consists of mainly three layers which are (Spiro OMe TAD), (CH₃NH₃PbI₃) and (SnO₂) as HTL, the absorber layer, and ETL with electron affinities of (-2.45, -3.9, and -3.75) eV respectively. Before investigating the influence of conduction

band offset on the perovskite solar cell parameters optimal doping and thickness of each layer of the proposed structure were achieved by parametric study. The results revealed that the doping of ETL and the thickness of the absorber plays a vital role in cell performance. The influence of layer doping and thicknesses of $\text{CH}_3\text{NH}_3\text{PbI}_3$ -based solar cells on different electrical parameters was examined. The absorber layer doping density ($> 10^{16} \text{ cm}^{-3}$) was found to be insufficient for high efficiency, whereas doping of acceptor in HTL ($> 10^{16} \text{ cm}^{-3}$) improved cell performance. The optimal absorber layer, HTL, and ETL values were 10^{14} cm^{-3} , 10^{19} cm^{-3} , and 10^{19} cm^{-3} , respectively. The optimized layer thickness values for the absorber layer, HTL, and ETL were 400 nm, 200 nm, and 300 nm, respectively, resulting in a higher power conversion efficiency of 24.19 percent with cell parameters of 26.1 mA cm^{-2} , 1.11 V, and 83.23 percent for the J_{sc} , V_{oc} , and FF. Formerly a thin layer of 3C-SiC was selected to use as an interfacial layer between the absorber layer and the ETL which produced spike-spike structure between the absorber and 3C-SiC layer and between the 3C-SiC layer and ETL based on the electron affinity of the ETL material produce a noticeable enhancement in J_{sc} and hence the PCE. That the spike offset between the 3C-SiC layer and ETL gives a better PSC performance. The obtained result of PCE was 28.36% for the proposed structure. Finally, the 3C-SiC layer improved the device performance by reducing the recombination at the border between the absorber layer and ETL.

References

- [1] D. Zhou, T. Zhou, Y. Tian, X. Zhu, and Y. Tu, "Perovskite-Based Solar Cells: Materials, Methods, and Future Perspectives," *J.Nanomater.*, vol. 20, 2018.
- [2] H. Kim, C. Lee, A. Marchioro and H. Moser, "Lead iodide perovskite sensitized all-solid-state submicron thin film mesoscopic solar cell with efficiency exceeding 9%," *Scientific reports*. Vol. 2, no. 1, pp1-7, 2012.
- [3] U. Sakee and M.Yin, "Highly compact TiO_2 layer for efficient hole - blocking in perovskite solar cells. *Applied Physics Express*," *Tetrahedron Lett.*, vol. 55, no. 5, pp. 3909, 2014.
- [4] Vivo P, Ojanperä A, Smått JH, Sandén S, Hashmi SG, Kaunisto K, Ihalainen P, Masood MT, Österbacka R, Lund PD, Lemmetyinen H, "Influence of TiO_2 compact layer precursor on the performance of perovskite solar cells," *Organic Electronics.*, vol. 41, pp. 287–293, 2017.



- [5] B. Peng, G. Jungmann, C. Jäger, D. Haarer, H. W. Schmidt, and M. Thelakkat, "Systematic investigation of the role of compact TiO₂ layer in solid state dye-sensitized TiO₂ solar cells," *Coord. Chem. Rev.*, vol. 248, no. 13–14, pp. 1479–1489, 2004.
- [6] M. Vasilopoulou, M. Fakharuddin and G. Coutsolelos, "Molecular materials as interfacial layers and additives in perovskite solar cells," *Chemical Society Reviews.*, vol. 49, no. 13, pp. 4496–4526, 2020.
- [7] Y. Gan, B. Xueguang, L. Yucheng and Q. Binyi, "Numerical Investigation Energy Conversion Performance of Tin-Based Perovskite Solar Cells Using Cell Capacitance Simulator," *Energies*. Vol. 5907, no 23, pp 768-772, 2020.
- [8] S. Ceills, Y. Wang, J. Wan, J. Ding, J. Hu, and D. Wang, "ARutile TiO₂ Electron Transport Layer for the Enhancement of Charge Collection for Efficient Perovskite Solar Cells," *Communications Solar Cells*. Vol 58, no. 26, pp 9414-9418, 2019.
- [9] D. N. Qasim Agha and Q. T. Algwari, "The influence of the interface layer between the electron transport layer and absorber on the performance of perovskite solar cells," *IOP Conf. Ser. Mater. Sci. Eng.*, vol. 1152, no. 1, p. 012033, 2021.
- [10] N. Lakhdar and A. Hima, "Electron transport material effect on performance of perovskite solar cells based on CH₃NH₃GeI₃," *Opt. Mater. (Amst)*, vol. 99, no.4, pp 104-109, 2020.
- [11] O. Shoewu, "Effect of Absorber Layer Thickness and Band Gap on the Performance of CdTe / CdS / ZnO Multi-Junction Thin Film Solar Cell," *International Journal of Advanced Tends in Technology*, vol. 4, no 7 pp20-26, 2018.
- [12] M. Mostefaoui, H. Mazari, S. Khelifi, A. Bouraiou, and R. Dabou, "Simulation of High Efficiency CIGS solar cells with SCAPS-1D software," *Energy Procedia*, vol. 74, pp. 736–744, 2015.
- [13] B. MariSoucase, I. G. Pradas, and K. R. Adhikari, "Numerical simulations on perovskite photovoltaic devices," *Perovskite Mater. Synth. characterisation, Prop. Appl.*, vol. 445, no. 33, pp 234-236 2016.
- [14] A. Hima, A. Khouimes, A. Rezzoug and M. Yahkem., "Simulation and optimization of CH₃NH₃PbI₃ based inverted planar heterojunction solar cell using SCAPS software," *International Journal of Energetica (IJECA)*. Vol. 4, no. 1, pp. 56-59, 2019.
- [15] A. Hima, N. Lakhdar, B. Benhaoua, and A. Saadoune, "An optimized perovskite solar cell designs for high conversion efficiency," *Superlattices Microstructures*. Vol. 129, no. 4, pp. 240–246, February 2019.
- [16] S. B. Naredla, "Electrical properties of molybdenum silicon carbide Schottky barrier diodes", 2019.
- [17] P. L. Zhou, S. K. Zheng, L. Ma, J. He, Y. Tian, and R. Shi, "Electronic and optical properties of Co-doped 3C-SiC from density functional calculations," *Solid State Commun* ", vol. 196, pp. 28–31, 2014.
- [18] B. Parida, J. Choi, G. Lim, K. Kim, and K. Kim, "Enhanced visible light absorption by 3C-SiC nanoparticles embedded in Si solar cells by plasma-enhanced chemical vapor deposition," *Journal Nanomater* "., vol. 2013, 2013.
- [19] A. Arvanitopoulos, N. Lophitis, K. Gyftakis, S. Perkins and M. Antoniou, "Validated physical models and parameters of bulk 3CSiC aiming for credible technology computer aided design (TCAD) simulation" *Semiconductor Science and Technology*. Vol.32, no.10, pp 104-109, 2017.
- [20] K. R. McIntosh, L. E. Black, K. R. McIntosh and L. E. Black, "On effective surface recombination parameters On effective surface recombination parameters," *Journal of Applied Physics*. Vol. 116, no. 1, pp 985-989, 2014.



- [21] Y. An, A. Shang, G. Cao and X. Li, “Perovskite Solar Cells : Optoelectronic Simulation and Optimization,” *Solae RRL*, vol. 2,no.11, pp 1800126, 2018.
- [22] U.andadapu, S.V.Vedanayakam, and K. Thyagarajan, “Simulation and Analysis of Lead based Perovskite Solar Cell using SCAPS-1D,” *Indian Journal of Science and Technology*, Vol 10, no.11, pp 346- 349, March, 2017.
- [23] S. Rahman, S. Miah, M. Sing, W. Marma, and T. Sabrina, “Simulation based Investigation of Inverted Planar Perovskite Solar Cell with All Metal Oxide Inorganic Transport Layers,” *Int. Conf.Electr. Comput. Commun. Eng.* Vol 12, no 6, pp. 453-458, 2019.
- [24]Y. Raoui, H. Ez-Zahraouy, S. Kazim, and S. Ahmad, “Energy level engineering of charge selective contact and halide perovskite by modulating band offset: Mechanistic insights,” *J. Energy Chem.*, vol.54, no. 1, pp. 822–829, 2021.
- [25] X. Zou, J. Cheng, C. Chang, Z. Zhou and Y. Yao, “Numerical simulation analysis of effect of energy band alignment and functional layer thickness on the performance for perovskite solar cells with Cd_{1-x}Zn_xS electron transport layer,” *Mater. Res. Express.* Vol. 7, no. 10, pp. 105906, 2020.